

Reflectometric Measurements of Fibre-based Orthogonal-pump FWM Systems

Hao Liu⁽¹⁾, Kyle R. H. Bottrill⁽¹⁾, Ali Masoudi⁽¹⁾, Valerio Vitali⁽¹⁾ and Periklis Petropoulos⁽¹⁾

⁽¹⁾Optoelectronics Research Centre, University of Southampton, SO17 1BJ, UK, hl1a18@soton.ac.uk

Abstract We experimentally demonstrate an optical time-domain reflectometry system with 50 cm spatial resolution, capable of measuring the onset of polarization dependency of orthogonal-pump four-wave mixing systems in the saturation regime. Close agreement with theoretical predictions is observed.
©2022 The Author(s)

Introduction

Four-wave mixing (FWM) processes, arising from Kerr nonlinearity in optical fibers, have enabled the demonstration of a large number of all-optical signal processing devices, such as wavelength converters^[1], phase-sensitive amplifiers^[2], amplitude and phase regenerators^{[3][4]}. There are two main approaches to achieve polarisation insensitive operation - polarisation diversity schemes and orthogonal pumping in non-degenerate FWM. In both of these approaches, residual birefringence in the nonlinear medium can lead to a polarisation dependent gain (PDG), degrading system performance. Although this effect can be mitigated in polarisation diversity schemes through the use of polarisation maintaining highly nonlinear fibre (HNLF), this option is not available in the orthogonal pump technique, wherein phase matching must be achieved on orthogonal polarisations at the same time. As such, studying the complex interplay between FWM and birefringence is essential if we are to perfect our control and understanding of such systems. By its nature, birefringence in lowly birefringent fibres varies along the length of the fibre in a stochastic process that is challenging both to measure and to model with accuracy. Ideally, a distance resolved measurement of the FWM process would help to understand the impact of birefringence and determine the accuracy of modelling. The use of optical time-domain reflectometry (OTDR) systems based on Rayleigh scattering is one solution to this problem, thanks to the possibility of measuring the spatial evolution of signals without disturbing the nonlinear processes.

The first use of OTDR to perform distributed FWM measurements in optical fibers was performed by Ravet et al^[5]. They studied the impact of dispersion in degenerate FWM in a dispersion-shifted fiber. More recently, a distributed mea-

surement of forward Brillouin scattering involving FWM processes was carried out in an 8 km-long single mode fiber for Brillouin-based fiber sensors^[6]. However, to the best of our knowledge, the orthogonally pumped FWM scheme and the dependence of its PDG on birefringence is yet to be explored.

In this work, we used an OTDR system to measure the Rayleigh back-scattered light of the phase conjugated idler generated by a forward FWM process. We initially validated the system by measuring the evolution of Rayleigh backscattered idler power in a dual, co-polarised pump scheme. The experimental results were compared with numerical simulations to confirm the accuracy of the modelling used. We then investigated the PDG in the orthogonal-pump FWM scheme, how it varies with the input signal's state

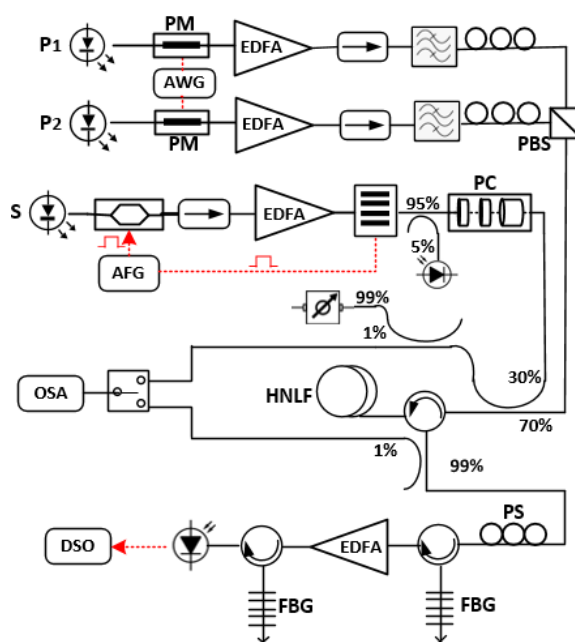


Fig. 1: OTDR-based orthogonal-pump FWM system setup; HNLF ($L = 500$ m; $\gamma = 11$ W⁻¹ · km⁻¹; $\beta_2=0.06$ ps/nm/km; $\beta_3=0.0035$ ps/nm²/km; $\alpha=1.44$ dB/km)

of polarization (SOP) and, in particular, how the onset of saturation affects PDG. Our results show that the onset of saturation depends upon the signal SOP and that saturation itself leads to strong increase in PDG.

Experimental setup

The experimental setup used for the distributed measurement of the phase conjugated idler generated in the orthogonal-pump FWM process is shown in Fig. 1. The signal generation stage was designed for polarisation stability and high ASE rejection, whilst the detection system has been designed to maximise sensitivity to the weakly Rayleigh backscattered light. Two continuous-wave (CW) laser sources, denoted as P1 and P2 in Fig. 1 (at wavelengths 1546.21 nm and 1552.61 nm), were used as the two pumps of the nonlinear process. To delay the onset of stimulated Brillouin scattering and reduce coherent Rayleigh noise (i.e. interference of backscattered light from different parts of pulse)^[7] in the HNLF, the linewidths of the two pumps were broadened through phase modulation. Two phase modulators were used for this purpose, which were driven by an 8 Gs/s, 2^{15} – 1-bit pseudo-random binary sequence (PRBS), generated from an arbitrary waveform generator (AWG) to obtain around 7 GHz bandwidth. A polarisation beam splitter (PBS) was used to ensure the polarisation states of the two pumps were orthogonal when launched into the HNLF. The signal in the FWM process was generated by a narrow linewidth laser ($\lambda = 1548.8$ nm), carved into a pulse train of 5 ns wide pulses with a repetition period of 15 μ s. This pulse duration enabled us to obtain OTDR traces with an approximately 50 cm spatial resolution. A programmable polarisation controller (PC) enabled measurements to be taken on each one of 64 different SOPs for the input signal. The signal was coupled together with the pumps in the HNLF by means of a 70:30 coupler. The Rayleigh backscattered light from the HNLF was then sent to a polarization scrambler (PS) (to remove any polarisation-dependent effects from the EDFA that followed), through a fibre Bragg grating (FBG) filter to reject the Rayleigh back-scattered light due to propagation of pump and signal. The filtered idler light was then amplified using an EDFA (to improve receiver sensitivity) before undergoing a final stage of filtering (to reject ASE from the EDFA), after which it was detected by a photodiode with transimpedance amplifier. A sys-

tematic description for all the optical components used in the signal pulse generation and receiving stages can be found in Ref^[8].

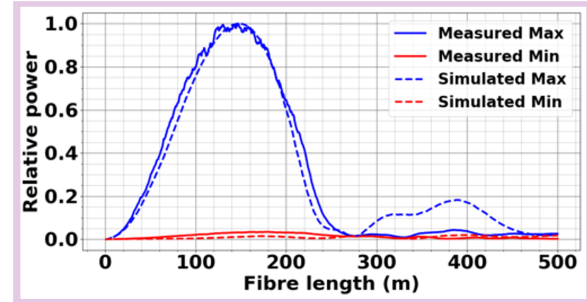


Fig. 2: Dual co-polarised pump FWM system; Measured maximum (solid trace in blue) and minimum (solid trace in red). Simulated maximum (dashed line in blue) and minimum (dashed line in red); total pump power: 952.2 mW; Peak signal power: 70.8 mW

Results and Discussion

The coupled Nonlinear Schrödinger Equation (C-NLSE) model^[9] was used to compare all the presented measurement results with numerical simulations by considering fibre parameters from the HNLF datasheet (reported in the caption of Fig. 1). Fibre birefringence was modelled using the Random Modulus Model (RMM)^[10], that allows fibres to be modelled with a birefringence that varies randomly along their length, determined by two parameters: the beat length L_b and the correlation length L_c . Since we are studying the trend of measured results, L_b and L_c were chosen to be 10 m and 100 m, which is a small perturbation for this fiber.

To confirm the correct functioning of the measuring system and the system's ability to measure sufficiently large PDG, we initially configured the system into the dual co-polarised pump scheme, which required only small modifications to be made to the system setup in Fig. 1. By varying the signal SOP, we measured both the case where the signal was co-polarised with the pumps (maximum conversion efficiency) and the case where it was orthogonal to the pumps (minimum conversion efficiency). As expected (Fig. 2), this latter SOP results in a strong suppression of the idler power, with a PDG of 13 dB measured about the peaks of the curves. A good agreement between experimental measurements and numerical simulation was found.

Finally, we used the system setup shown in Fig. 1 to perform a distributed characterization of the orthogonal-pump FWM system. Three different pump power levels (total pump power of 374 mW, 574 mW and 1105 mW, respectively) were used to measure the polarisation dependency of the

idler as the signal SOP was varied. The resultant curves show that both the saturated idler power and the distance along the fibre at which saturation is reached vary with signal SOP. We can, therefore identify the curves with 1) the maximum saturated idler power, 2) the minimum saturated idler power and 3) the earliest onset of saturation along the fibre length for different pump power levels. This procedure was carried out for both the experimental measurements and the numerical results and good agreement can be seen between them for all three pump power cases studied. It needs to be noted that traces with the same color in Fig.3(a-c) have the same input signal SOP.

The simulation indicates that saturation occurs soonest when the signal has a SOP that is 45° relative to the two orthogonal pumps. Therefore, in the experiment, we identify the curve that saturates the soonest as possessing this 45° relative polarisation. Amongst the results are traces with differing shapes, breadth and flatness, evidence of a rich variation which could be exploited for other purposes, such as improved squeezing performance in saturation based amplitude limiters.

In Fig. 3(d), a plot of PDG as it evolves along the length of the fibre is presented, obtained by taking the difference between the maximum and minimum idler power measurement values from the 64 polarisation states. These data show that saturation of the FWM process is associated with an increase in PDG and should therefore be avoided for most applications. As expected, as pump power increases, the onset of saturation is met earlier in the fibre and hence PDG begins to grow sooner. The numerical simulations predicted the same onset distance as the experimental results, further supporting the modelling. The discrepancy between numerical and experimental plots before 200 m is attributed to the low SNR at the beginning of the fiber, which limits the lowest measurable PDG value to around 1.5 dB.

Conclusions

We demonstrated an OTDR-based characterisation of an orthogonal-pump FWM system, capable of measuring the polarisation dependency of a Rayleigh backscattered idler. The saturation regime for the idler power was investigated considering different pump power levels and input signal SOPs. A good matching between numerical simulations and experimental results was found considering the extreme cases of maxi-

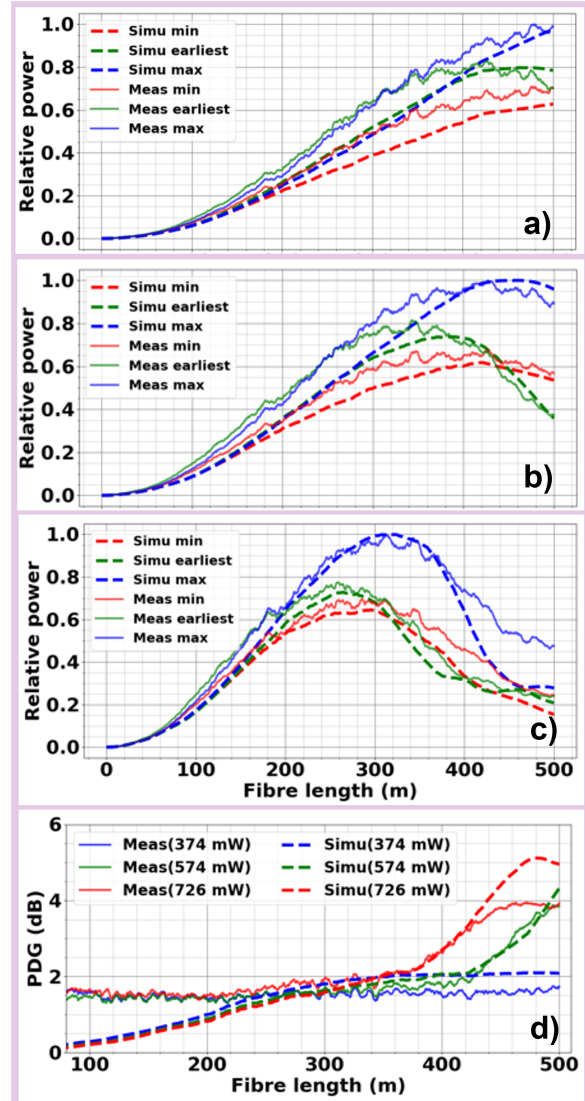


Fig. 3: Measured and simulated minimum (solid trace and dashed line in red), maximum (solid trace and dashed line in blue) and earliest (solid trace and dashed line in green) idler saturation curves of using (a) 374 mW, (b) 574 mW and (c) 1105 mW total pump power; The input signal peak power is fixed at 108 mW; (d) Measured (solid trace) and simulated PDG (dashed line) evolution curve for three different total pump power levels shown in the legend

mum, minimum and earliest saturation curves. This system would help us to avoid saturation when designing wavelength converters and also help us to exploit it when designing saturation based amplitude limiter. Moreover, we believe that the confirmation of the model's reliability and the performance of the measurement scheme will allow further in-depth study into the complex effect that birefringence has on FWM systems.

Acknowledgements

This work was supported by the UK's EPSRC through grant EP/S002871/1. The data for this work is accessible through the University of Southampton Institutional Research Repository DOI:10.5258/SOTON/D2213.

References

- [1] S. Watanabe, T. Kato, T. Tanimura, *et al.*, "Wavelength conversion using fiber cross-phase modulation driven by two pump waves", *Optics express*, vol. 27, no. 12, pp. 16 767–16 780, 2019. DOI: 10.1364/OE.27.016767.
- [2] P. A. Andrekson and M. Karlsson, "Fiber-based phase-sensitive optical amplifiers and their applications", *Advances in Optics and Photonics*, vol. 12, no. 2, pp. 367–428, 2020. DOI: 10.1364/AOP.382548.
- [3] F. Parmigiani, G. Hesketh, R. Slavík, P. Horak, P. Petropoulos, and D. J. Richardson, "Polarization-assisted phase-sensitive processor", *Journal of Lightwave Technology*, vol. 33, no. 6, pp. 1166–1174, 2015. DOI: 10.1109/JLT.2014.2385598.
- [4] K. R. Bottrill, N. Taengnoi, Y. Hong, D. Richardson, and P. Petropoulos, "Phase preserving amplitude saturation through tone synthesis assisted saturated four-wave mixing", *Journal of Lightwave Technology*, vol. 38, no. 7, pp. 1817–1826, 2020. DOI: 10.1109/JLT.2020.2973593.
- [5] G. Ravet, F. Vanholsbeek, P. Emplit, M. Wuilpart, and P. Mégret, "Otdr technique for the characterization of fwm processes in optical fibers", in *IEEE Laser and Electro-Optics Society Symposium*, 2007, pp. 203–206.
- [6] Y. London, H. H. Diamandi, G. Bashan, and A. Zadok, "Invited article: Distributed analysis of nonlinear wave mixing in fiber due to forward brillouin scattering and kerr effects", *APL Photonics*, vol. 3, no. 11, p. 110 804, 2018. DOI: 10.1063/1.5042635.
- [7] A. Masoudi and T. P. Newson, "Analysis of distributed optical fibre acoustic sensors through numerical modelling", *Optics express*, vol. 25, no. 25, pp. 32 021–32 040, 2017. DOI: 10.1364/OE.25.032021.
- [8] A. Masoudi, M. Beresna, and G. Brambilla, "152 km-range single-ended distributed acoustic sensor based on inline optical amplification and a micromachined enhanced-backscattering fiber", *Optics Letters*, vol. 46, no. 3, pp. 552–555, 2021. DOI: 10.1364/OL.413206.
- [9] M. Marhic, A. Rieznik, G. Kalogerakis, C. Braimiotis, H. Fragnito, and L. Kazovsky, "Accurate numerical simulation of short fiber optical parametric amplifiers", *Optics express*, vol. 16, no. 6, pp. 3610–3622, 2008. DOI: 10.1364/OE.16003610.
- [10] W. Huang and D. Yevick, "Polarization mode dispersion in short fiber lengths", *JOSA A*, vol. 23, no. 6, pp. 1509–1512, 2006. DOI: 10.1364/JOSAA.23.001509.